



# Variations and Source Apportionment of PM<sub>2.5</sub> and PM<sub>10</sub> Before and During COVID-19 Lockdown Phases in Delhi, India

S. Fatima<sup>1,2</sup>, A. Ahlawat<sup>3</sup>, S. K. Mishra<sup>1,2\*</sup>, M. Maheshwari<sup>4</sup> and V. K. Soni<sup>5</sup>

<sup>1</sup>CSIR-National Physical Laboratory, New Delhi 110012, India

<sup>2</sup>Academy of Scientific and Innovative Research (AcSIR), Ghaziabad, Uttar Pradesh 201002, India

<sup>3</sup>Leibniz Institute for Tropospheric Research (TROPOS), Permoserstraße, 04318 Leipzig, Germany

<sup>4</sup>Amity University, Noida 201301, India

<sup>5</sup>India Meteorological Department, Ministry of Earth Sciences, New Delhi 110003, India

Received: 28 February 2021 / Accepted: 05 September 2021

© Metrology Society of India 2021

**Abstract:** Major cities across the globe including megacity Delhi have experienced considerable lower levels of air pollutants including particulate matter (PM) during COVID-19 lockdown. This study explores pre-lockdown and during lockdown air quality changes in PM<sub>2.5</sub>, PM<sub>10</sub>, PM<sub>2.5</sub>/PM<sub>10</sub> ratio along with meteorological effects. Selected sites with different pollution signatures in Delhi including Alipur (residential), Okhla (industrial) and Pusa Road (traffic) have experienced mean (S.D.) PM<sub>2.5</sub> as 87.56(± 54.06), 124.45(± 73.49) and 62.14(± 58.64) µg/m<sup>3</sup> and PM<sub>10</sub> as 163.01(± 77.37), 217.71(± 93.94) and 135.15(± 77.90) µg/m<sup>3</sup> before lockdown (BL), while for Lockdown 1 (L1), PM<sub>2.5</sub> concentrations decreased drastically as 39.26(± 16.31), 38.01(± 15.16) and 31.03(± 12.79) µg/m<sup>3</sup> and for PM<sub>10</sub> as 100.76(± 43.71), 79.47(± 30.97) and 66.53(± 22.78) µg/m<sup>3</sup>, respectively, with gradual increase in both pollutants during successive lockdown phase—Lockdown 2, Lockdown 3, Lockdown 4 and Unlock phase 1. The percentage (%) decrease in PM<sub>2.5</sub> (69.46%) and PM<sub>10</sub> (63.49%) during lockdown was found well correlated with people mobility (Google and Apple mobility reports), as outdoor activities showed 70–80% decrease in L1 from BL phase. Source apportionment studies suggested both local and regional pollution contribution in Delhi. Comparison of PM<sub>2.5</sub> and PM<sub>10</sub> concentrations for the year 2020 with that of 2018 and 2019 and study on diurnal variations of PM<sub>2.5</sub> and PM<sub>10</sub> have been discussed.

**Keywords:** PM<sub>2.5</sub>; PM<sub>10</sub>; PM<sub>2.5</sub>/PM<sub>10</sub> ratio; COVID-19"/>

## 1. Introduction

The novel coronavirus outbreak for SARS-CoV-2 variant took place at a very fast rate during COVID-19 pandemic. This variant of coronavirus was firstly detected during December 2019 in Wuhan City of China. COVID-19 was declared as a pandemic event in March 2020 by World Health Organization [1]. On 30 September 2020, global confirmed COVID-19 number of cases was 34,084,559, including 1,016,517 deaths reported from N200 countries/territories worldwide [2]. As per studies reported, six metropolitan cities in India including Delhi, Mumbai, Kolkata, Ahmedabad, Pune and Chennai have known to

account, approximately 50% of total reported COVID-19 cases, all over India [3]. COVID-19 lockdown has caused serious reduction in air pollution status across the globe [4–6]. Primary air pollutants (gaseous + particulates) reduction have also been experienced in the Eastern parts of China as a result of adverse effects of meteorological conditions on air pollutants during COVID-19 [7]. As per previous studies, poor air quality of Chinese cities has been found in linkage with higher rate of mortality within those cities [8], whereas lockdown conditions have also been associated with lower pre-mature deaths in some cities as a result of air quality up-gradation during COVID-19 [9, 10]. According to a study in China, a significant relationship has been found between air pollution and infection due to COVID-19 virus among people [11]. In New York, USA, meteorological parameters like average and minimum

\*Corresponding author, E-mail: sumitkumarm@gmail.com

temperature, and air quality changes have been known to be linked with effects due to COVID-19 pandemic [12]. According to the reported studies, lower levels of air pollutants were experienced in Barcelona, Spain, during COVID-19 lockdown [13]. In India, metropolitan cities with heavy crowd including Delhi, Mumbai, Kolkata and Bangalore have experienced lower concentrations levels of major air pollutants with significant improvement in their respective air quality during lockdown conditions, in comparison with before lockdown air quality conditions [14, 15].

Ambient atmosphere carries PM of different sizes with their distinct characteristics and causes adverse effects due to their variable chemical compositions, physical characteristics, site location and types of emission sources [16, 17]. Fine particles like  $PM_{2.5}$  (particulate matter with diameters less than  $2.5 \mu m$ ) and coarse particles like  $PM_{10}$  (particulate matter with diameters less than  $10 \mu m$ ) are most common sizes of particulate matter found in the ambient atmosphere and are of major concern related to research studies. Sources for coarse particles ( $PM_{2.5}$  to  $PM_{10}$ ) include re-suspension of loose soil or road dust, natural dust storms and different industrial processes [18], whereas fine particles ( $PM_{2.5}$ ) sources include emissions from heavy traffic activities, energy production processes, biomass burning, etc. [19]. Factors like variable meteorological conditions, land use patterns and population density cause spatio-temporal variations in PM concentrations and other pollutants at both local and regional levels [20, 21].

Since both fine and coarse particles have different physico-chemical properties and diverse sources of emissions/generations, the  $PM_{2.5}/PM_{10}$  ratio plays a crucial role in providing information related to particulate matter's origin, their formation processes and thus providing a base to study their associated negative health effects [22, 23]. A higher value for  $PM_{2.5}/PM_{10}$  ratio shows dominance of fine particles mainly emitted from anthropogenic sources, whereas, smaller  $PM_{2.5}/PM_{10}$  ratio reveals dominance of coarse particles mainly generated from natural sources including road-dust suspension, natural dust storm, etc. [24]. The values of this ratio show greater spatial variations indicating heterogeneity of  $PM_{2.5}/PM_{10}$  ratio at different regions as an effect of variable meteorological conditions at different places [25, 26]. Higher  $PM_{2.5}/PM_{10}$  ratio during winters has been reported [27], due to meteorological parameters including less rainfall or precipitation conditions, low temperature, lower boundary layer depth and stable atmospheric conditions which limit  $PM_{2.5}$  dispersion in ambient atmosphere [25, 26, 28].

Higher levels of both  $PM_{2.5}$  and  $PM_{10}$ , found in the ambient atmosphere of Delhi, much more than the standards limits set by the National Ambient Air Quality Standards (NAAQS), India [15, 29]. COVID-19 pandemic

in India led to a nationwide lockdown starting from 24 March till 31 May 2020. This nationwide lockdown caused a decreased industrial activities and lesser transportation activities due to which pre-lockdown pollution level of different pollutants, decrease drastically during lockdown event in India [15, 30–33]. Therefore, the present work explores the air quality changes in fine and coarse particulate matter (PM) at different sites of Delhi having different pollution signatures, before lockdown, during different lockdown and unlock phases in Delhi, India.

The objectives of the present study include:

- (i) Variations in concentrations of  $PM_{2.5}$ ,  $PM_{10}$ ,  $PM_{2.5}/PM_{10}$  ratio and meteorological parameters within different site characteristics (Alipur, Okhla and Pusa Road) in Delhi, India, before lockdown and during different phases of lockdown and unlock phases;
- (ii) Source apportionment studies to find major reasons for the PM level variations within Delhi, before lockdown and during different phases of lockdown and unlock phases.
- (iii) Comparisons of PM ( $PM_{2.5}$  and  $PM_{10}$ ) variations (2020) with that of year 2018 and 2019 and comparison of PM diurnal variations (2020) during various lockdown phases (BL, L1, L2, L3, L4, UL1).

## 2. Materials and Methods

### 2.1. Site Description

Delhi has been chosen as study area which is the capital city of India and lies at Indo-Gangetic Plains (IGP). Delhi covers an area of  $\sim 1485 \text{ km}^2$  (Coordinates- Latitude:  $28^{\circ}36'36''N$ ; Longitude:  $77^{\circ}13'48''E$ ) (Fig. 1). Delhi is a semi-arid zone having typical IGP climate with four major seasons: pre-monsoon (Mar–May), monsoon (Jun–Sept), post-monsoon (Oct–Nov) and winter (Dec–Feb) seasons. Traffic density, industrial activities, construction works, dust re-suspension, biomass burning, regional transport of pollutants are major contributors of particulate matter ( $PM_{2.5}$  and  $PM_{10}$ ) in Delhi, India. Present study includes three representative sampling sites—Alipur as rural, Okhla as Industrial and Pusa Road as Traffic with residential area (Fig. 1).

### 2.2. Data Collection and Analysis

Real-time data for  $PM_{2.5}$  and  $PM_{10}$  was collected from air quality monitoring stations (For three sampling sites—Alipur, Okhla and Pusa Road) which have been installed and being monitored in collaboration with CPCB (continuous ambient air quality monitoring, CAAQM and manual

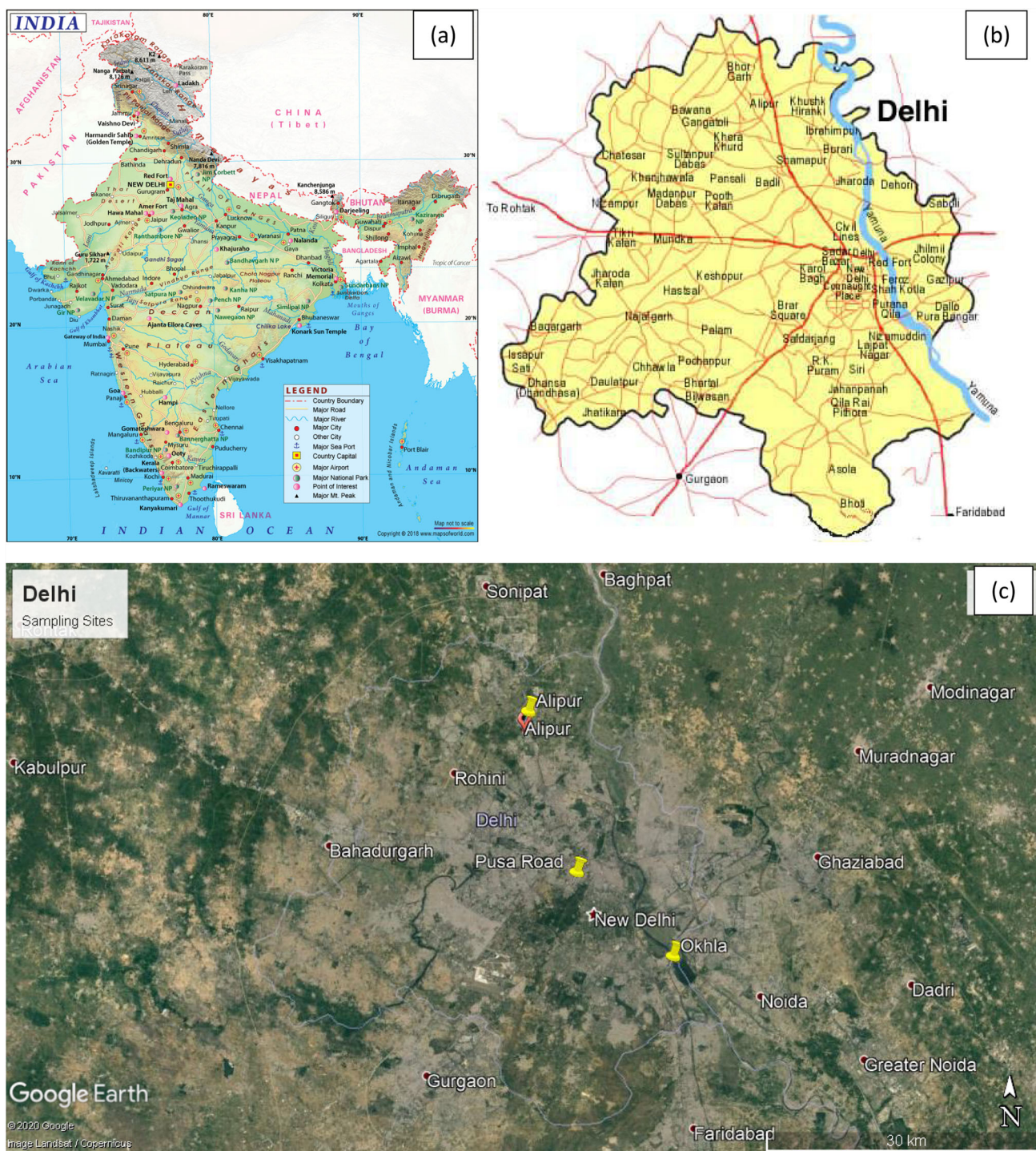


**Fig. 1** a Political map of India. b Map of Delhi, India. c Google Earth image showing location of selected sampling sites

ambient air quality monitoring, MAAQM); DPCC (Delhi Pollution Control Committee); IITM (Indian Institute of Tropical Meteorology), Pune; and, SAFAR (System of Air Quality and Weather Forecasting and Research). The collected data has been converted into daily average data for concentrations ( $\mu\text{g}/\text{m}^3$ ) of PM<sub>2.5</sub>, PM<sub>10</sub> and meteorological parameters including wind direction, wind speed,

temperature and relative humidity. The raw data used here, is available at CPCB online portal for air quality data dissemination [34] which has been analysed for air quality assessment studies for before and during the different lockdown periods of COVID-19 and unlock phases. The data follow quality assurance or quality control (QA/QC) protocols which is done by CPCB using rigorous protocols

**Table 1** Mean values of relative humidity, air temperature, wind speed, PM<sub>2.5</sub>, PM<sub>10</sub> and PM<sub>2.5</sub>/PM<sub>10</sub>, during different lockdown and unlock phases (BL, L1, L2, L3, L4 and UL1) in Delhi

Sampling locations	Phases/ events	Mean relative humidity (RH %)	Mean atmospheric temperature (AT in °C)	Mean wind speed (WS in m/s)	Mean PM <sub>2.5</sub> (ug/m <sup>3</sup> )	Mean PM <sub>10</sub> (ug/m <sup>3</sup> )	Mean PM <sub>2.5</sub> /PM <sub>10</sub> ratio
Alipur	Before lockdown (BL)	61.17 (± 5.92)	18.48 (± 3.97)	1.16 (± 0.05)	87.56 (± 54.06)	163.01 (± 77.37)	0.54 (± 0.10)
Okhla		66.57 (± 11.87)	17.54 (± 3.72)	0.82 (± 0.32)	124.45 (± 73.49)	217.71 (± 93.94)	0.54 (± 0.11)
Pusa Road		58.10 (± 9.16)	23.52 (± 3.96)	1.32 (± 1.00)	62.14 (± 58.64)	135.15 (± 77.90)	0.48 (± 0.10)
Alipur	Lockdown 1 (L1)	50.08 (± 7.34)	24.94 (± 2.78)	1.16 (± 0.05)	39.26 (± 16.31)	100.76 (± 43.71)	0.40 (± 0.08)
Okhla		42.05 (± 11.89)	27.21 (± 2.77)	0.86 (± 0.27)	38.01 (± 15.16)	79.47 (± 30.97)	0.48 (± 0.07)
Pusa Road		51.45 (± 8.92)	25.85 (± 2.57)	1.89 (± 0.68)	31.03 (± 12.79)	66.53 (± 22.78)	0.47 (± 0.12)
Alipur	Lockdown 2 (L2)	44.99 (± 5.69)	28.66 (± 1.78)	1.16 (± 0.04)	50.72 (± 18.36)	147.24 (± 47.69)	0.34 (± 0.08)
Okhla		41.36 (± 11.93)	29.87 (± 2.09)	0.75 (± 0.17)	43.15 (± 14.54)	107.92 (± 36.22)	0.40 (± 0.09)
Pusa Road		46.77 (± 7.81)	28.39 (± 3.46)	1.20 (± 0.67)	49.35 (± 36.57)	101.92 (± 54.53)	0.44 (± 0.12)
Alipur	Lockdown 3 (L3)	45.63 (± 4.64)	30.12 (± 1.55)	1.23 (± 0.03)	65 (± 20.45)	136.12 (± 42.97)	0.48 (± 0.04)
Okhla		41.70 (± 10.13)	31.33 (± 2.04)	0.77 (± 0.18)	46.42 (± 14.30)	114.37 (± 30.96)	0.40 (± 0.05)
Pusa Road		46.86 (± 8.39)	31.20 (± 3.12)	2.21 (± 1.42)	57.01 (± 14.02)	115.64 (± 21.57)	0.49 (± 0.09)
Alipur	Lockdown 4 (L4)	38.40 (± 10.69)	33.05 (± 3.51)	1.23 (± 0.03)	68.43 (± 35.12)	180.90 (± 76.68)	0.39 (± 0.13)
Okhla		30.69 (± 21.50)	34.87 (± 4.21)	0.90 (± 0.30)	47.46 (± 24.40)	153.21 (± 62.84)	0.32 (± 0.11)
Pusa Road		41.24 (± 12.95)	34.00 (± 3.82)	2.58 (± 1.26)	46.03 (± 23.97)	132.10 (± 51.52)	0.36 (± 0.12)
Alipur	Unlock 1 (UL1)	51.18 (± 3.79)	32.32 (± 2.82)	1.27 (± 0.09)	51.05 (± 11.58)	120.16 (± 36.60)	0.36 (± 0.08)
Okhla		54.72 (± 5.72)	32.33 (± 2.54)	0.54 (± 0.13)	46.66 (± 10.63)	135.59 (± 45.92)	0.42 (± 0.08)
Pusa Road		51.27 (± 4.51)	33.43 (± 2.77)	1.83 (± 0.51)	39 (± 10.52)	94.70 (± 30.55)	0.44 (± 0.06)

for the calibration of the instruments. Data from January to June 2020 have been studied for analysing air quality before and during different COVID-19 lockdown and unlock phases as mentioned below:

Different phases of lockdown and unlock during COVID-19

Before lockdown (BL): 1 January–24 March 2020 (~ 3 months);

Lockdown phase-1 (L1): 25 March–14 April 2020 (21 days);

Lockdown phase-2 (L2): 15 April–3 May 2020 (19 days)

Lockdown phase-3 (L3): 4 May–17 May 2020 (14 days);

Lockdown phase-4 (L4): 18 May–31 May 2020 (14 days);

Unlock phase-1.0 (UL1): 1 June–30 June 2020 (30 days; data analysis done for 20 days).

Percentage (%) change is calculated by using following formula (e.g. % change for BL–L1):

$$((BL - L1)/BL) * 100.$$

Here, percentage (%) change is calculated for L1 with respect to BL phase.

**Table 2** Percentage (%) change of PM<sub>2.5</sub> and PM<sub>10</sub> during lockdown and unlock phases with that of before lockdown conditions (BL)

	Alipur		Okhla		Pusa Road	
	PM <sub>2.5</sub>	PM <sub>10</sub>	PM <sub>2.5</sub>	PM <sub>10</sub>	PM <sub>2.5</sub>	PM <sub>10</sub>
BL–L1	55.16	38.19	69.46	63.50	50.06	50.77
BL–L2	42.07	9.67	65.33	50.43	20.58	24.59
BL–L3	25.77	16.50	62.70	47.47	8.26	14.44
BL–L4	21.85	– 10.97	61.86	29.63	25.93	2.26
BL–UL1	41.70	26.29	62.51	37.72	37.24	29.93

For each phase (L1, L2, L3, L4, UL1), + ve values correspond to % decrease and – ve values correspond to % increase, w.r.t BL

Data for human mobility trends have been obtained from Google Mobility Reports and Apple Mobility Reports. Wind Trajectories have been obtained using NOAA HYSPLIT Trajectory model [35], and fire count data have been obtained using NASA's MODIS active fire data ([36]; Figure Courtesy-[37]). NASA's Fire Information for Resource Management System (FIRMS) used here provides fire maps for specific dates on global location to confirm biomass burning activities. NOAA HYSPLIT Trajectory Model used here provides maps for back trajectories for wind which shows contribution of local and regional polluting sources at a specific location.

### 3. Results and Discussion

#### 3.1. Measurements of Surface Meteorology

Variations in surface meteorology for meteorological parameters including relative humidity (%), atmospheric temperature (°C) and wind speed (m/s) are provided in Table 1 for all the three sampling sites for different phases of BL, L1, L2, L3, L4 and UL1. Highest mean relative humidity (R.H.) is observed during before lockdown phase whereas lowest during L4 phase at all the three sampling sites. Air temperature (°C) is found lowest during before lockdown phase and highest during L4 phase. The reason behind this is average values of before lockdown phase also consists of winter season values whereas other lockdown phases and L4 have predominantly summer season with higher temperature and lower R.H. values. At both Okhla and Pusa Road, highest average wind speed has been observed during L4 phase whereas for Alipur it is observed during UL1 phase. Higher wind speed helps in dispersion of pollutants and lower wind speed causes accumulation of pollutants within a specific area.

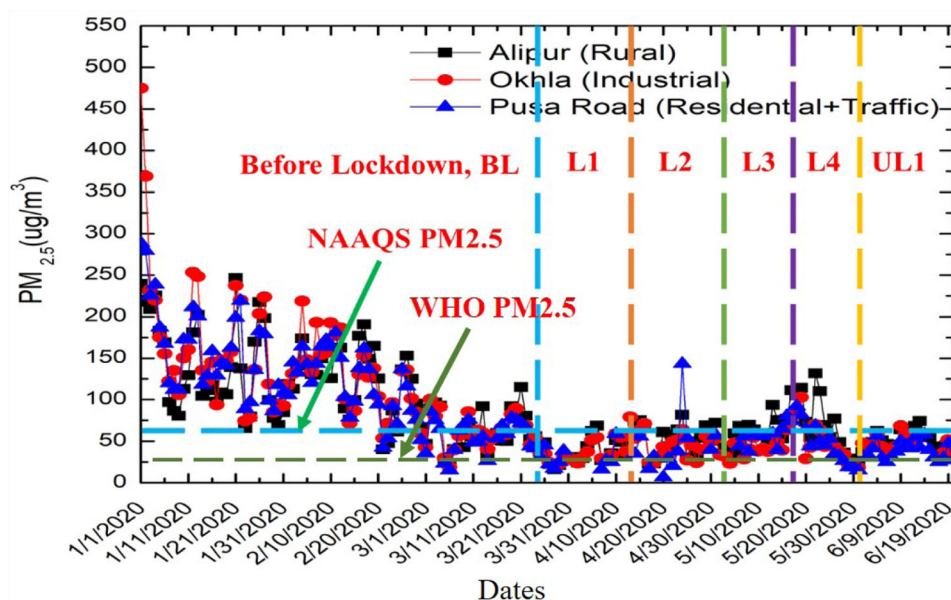
It is reported that lower temperature plays a major role in pollution build-up due to lower boundary layer during winters while higher relative humidity during winters leads to secondary aerosol particle formation, increasing the PM concentrations [38, 39]. Recent studies have revealed that

cold and dry conditions were found to accelerate the rate of coronavirus spread [40–46] and decrease in relative humidity leads to an increase in viral spread [47–49]. The coronavirus is found less airborne active in hot and humid conditions [50]. Therefore, the climatic condition with lower R.H. in Delhi, has more transmission potential for the coronavirus spread among residents and during winters, the COVID-19 virus spread is presumed to spread with faster rate due to colder temperature, whereas the virus spread will be lower during hot and dry conditions of summer.

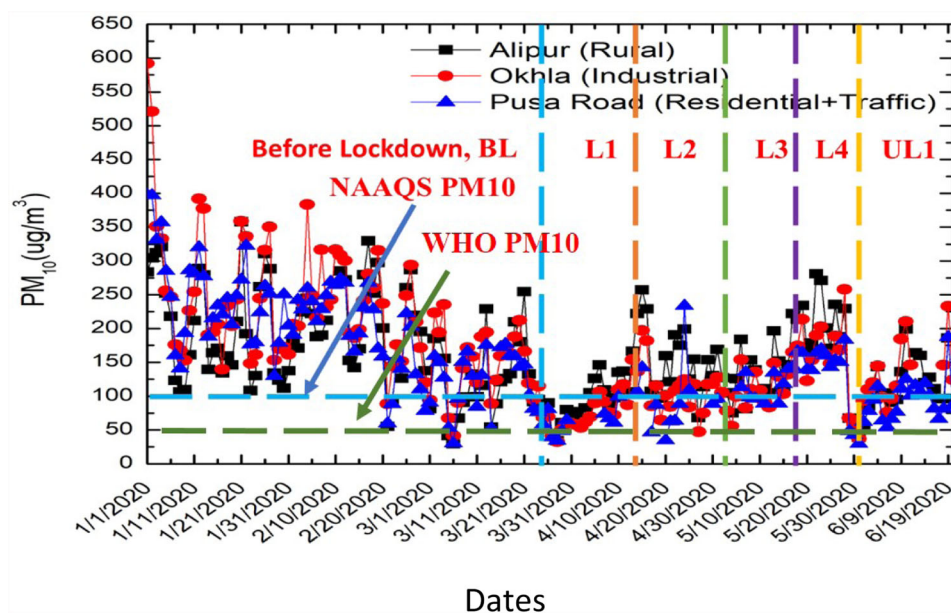
#### 3.2. Variations in PM<sub>2.5</sub> and PM<sub>10</sub> Before and During COVID-19 Lockdown

Table 1 shows mean values for PM<sub>2.5</sub> and PM<sub>10</sub> concentrations. Highest mean values for concentrations (µg/m<sup>3</sup>) were reported for both PM<sub>2.5</sub> and PM<sub>10</sub>, before lockdown phase while lowest values were reported during L1 Phase, at all the three sampling sites. The reason for the difference in these concentrations' values is due to higher emissions of PM before COVID-19 lockdown and sudden decrease in emitting sources due to COVID-lockdown conditions. For pre-COVID concentrations, Okhla reported highest values for PM<sub>2.5</sub> and PM<sub>10</sub> due to industrial emissions, followed by Alipur due to vehicular emissions at national highway and biomass burning activities in nearby agricultural fields and landfill waste burning, and then Pusa Road due to traffic emissions. Similar studies have shown effect of COVID-19 lockdown on the reduced concentrations of air pollutants in Delhi and other parts of India [30, 31, 33].

After L1 phase, both PM<sub>2.5</sub> and PM<sub>10</sub> concentrations found gradual increasing for L2, L3 and L4 phases as slight relaxation of lockdown measures was observed after L1 phase (from 7 April 2020) for both vehicular movement and industrial processes and functioning, beyond the red zone (government recognized infected zone from major COVID-19 cases) (Figs. 2, 3). For unlock phase (UL1), due to rainy events occurred in monsoon season, concentrations for both pollutants decreased even after visible movements of residents. PM<sub>2.5</sub> and PM<sub>10</sub> have reduced below the



**Fig. 2** Daily variations in  $PM_{2.5}$  concentrations for three different sites identified by their region-specific signatures: **a** Alipur, **b** Okhla, **c** Pusa Road before, during and after lockdown phases



**Fig. 3** Daily variations in  $PM_{10}$  concentrations for three different sites identified by their region-specific signatures: **a** Alipur, **b** Okhla, **c** Pusa Road before, during and after lockdown phases

NAAQS permissible limit set by CPCB, at all the three sites during L1 and increased for some days during L2, L3, L4 and UL1 (Figs. 2, 3). However,  $PM_{2.5}$  and  $PM_{10}$  concentrations were found reduced below WHO standard limit on very few days during lockdown phases (Figs. 2, 3). The present study showed mean concentrations (Standard deviations; S.D.) at all the three selected sampling sites—

Alipur, Okhla, Pusa, for  $PM_{2.5}$  as  $87.56 (\pm 54.06)$ ,  $124.45 (\pm 73.49)$  and  $62.14 (\pm 58.64) \mu\text{g}/\text{m}^3$  and for  $PM_{10}$  as  $163.01 (\pm 77.33)$ ,  $217.71 (\pm 93.94)$  and  $135.15 (\pm 77.90) \mu\text{g}/\text{m}^3$  before lockdown (BL), while both  $PM_{2.5}$  and  $PM_{10}$  concentrations were drastically decreased during (Lockdown-1 phase) L1 (Table 1). For L1,  $PM_{2.5}$  concentrations were reported as  $39.26 (\pm 16.31)$ ,  $38.01 (\pm 15.16)$  and

31.03 ( $\pm 12.79$ )  $\mu\text{g}/\text{m}^3$  while for PM<sub>10</sub> as 100.76 ( $\pm 43.71$ ), 79.47 ( $\pm 30.97$ ) and 66.53 ( $\pm 22.78$ )  $\mu\text{g}/\text{m}^3$  with gradual increase in concentrations for both pollutants at all the three sampling sites during successive lockdown phases including L2, L3, L4 and unlock phase—UL1 (Table 1; Figs. 2, 3). PM<sub>2.5</sub> percentage (%) change from BL–L1, L1–L2, L2–L3, L3–L4, L4–UL1 is calculated as – 55.16, 29.19, 28.15, 5.28, – 25.39 for Alipur, – 69.46, 13.52, 7.58, 2.24, – 1.68 for Okhla and – 31.11, 59.04, 15.52, – 19.26, – 15.27 for Pusa Road, respectively. Also, PM<sub>10</sub> percentage (%) change from BL–L1, L1–L2, L2–L3, L3–L4, L4–UL1 is calculated as – 38.19, 46.13, – 7.55, 32.90, – 33.58 for Alipur, – 63.50, 35.80, 5.98, 33.96, 11.50 for Okhla and – 50.77, 53.19, 13.46, 14.23, – 28.31 for Pusa Road site, respectively. Srivastava et al. [31] have reported percentage (%) decrease of ~ 58% and 47% in PM<sub>10</sub> and PM<sub>2.5</sub> concentration, respectively, in Delhi. Highest percentage (%) decrease at Okhla industrial site than other sites during lockdown period shows lesser industrial activities during the period whereas almost 50% decrease in PM concentrations at Pusa Road may be due to lesser traffic activities during lockdown period and percentage (%) decrease in PM concentrations, particularly PM<sub>10</sub>, at Alipur may be attributed to somewhat lower but ongoing rural activities, landfill burnings, agricultural burnings but decrease in vehicular emissions at local roads and nearby national highways. Percentage (%) change of PM for L1, L2, L3, L4 and UL1 conditions with that of BL is shown in Table 2. This table also confirms the above discussions along with the fact that at Alipur site percentage (%) decrease of 55.16% in BL–L1 shows half cut in PM<sub>2.5</sub> sources as an effect of sudden lockdown conditions while – 10.97% increase in PM<sub>10</sub> in BL–L4 shows effect of dust-storms and biomass burning activities. More than half cut (> 60% decrease) in PM<sub>2.5</sub> emissions is

attributed to lower/closed industrial activities as Okhla site. At Pusa Road site percentage (%) decrease in PM<sub>2.5</sub> and PM<sub>10</sub> in BL–L1 shows the effect of lockdown activities with lower traffic emission and road-dust suspension and lesser % decrease in PM<sub>2.5</sub> by only 8.26% in BL–L3 shows effect of biomass burning activities and lenient lockdown rules. PM<sub>10</sub> concentrations for Alipur also remained highest among other sites, during the whole lockdown period despite being rural area which may be due to the mentioned ongoing localized activities like agricultural burning, landfill burning, road-dust suspension, dust-storm events, etc. (Fig. 3). Higher PM<sub>2.5</sub> concentrations values at rural area of Alipur during L3 and L4 and fire count data confirms crop burning events at localized and regional areas nearby Delhi (Figs. 2, 10).

According to human mobility trend reports including Google mobility reports [51] and Apple mobility reports [52] (Figs. 4, 5), % increase in people mobility trend showed ~ 40% increase during L1, L2, L3 and ~ 30% increase during L4 and UL1, in residential activities with respect to before lockdown phase. Outdoor activities like visiting grocery stores, retails, parks, transit stations and workplaces have decreased during L1 (70–80%) and gradually increased in successive phases of lockdown and unlock phases with up to – 20% t during UL1 phase (Figs. 4, 5). This shows majority of Delhi residents were inside their homes during lockdown phases while some residents went to buy essentials and groceries, personal works and in transit for meeting their family members living nearby or migrating to places. Also, with the successive lockdown phases, outdoor activities increased but significant number of people were found to be associated with residential activities. The gradual increase in both PM<sub>2.5</sub> and PM<sub>10</sub> concentrations was found well correlated with people mobility during different lockdown phases

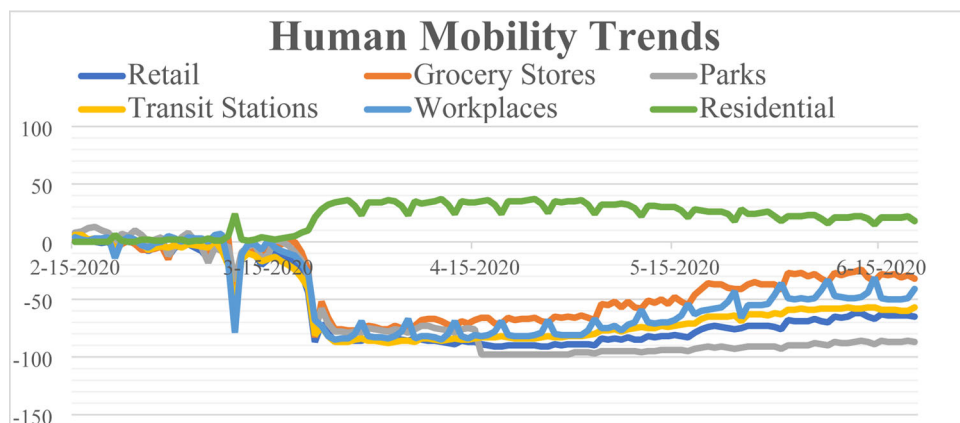


**Fig. 4** Human mobility report for Delhi, India, from 15.02.2020 to 20.06.2020 for different places such as retail, grocery stores, parks, transit stations, workplaces and residential complexes. (Google Mobility Reports, [51])

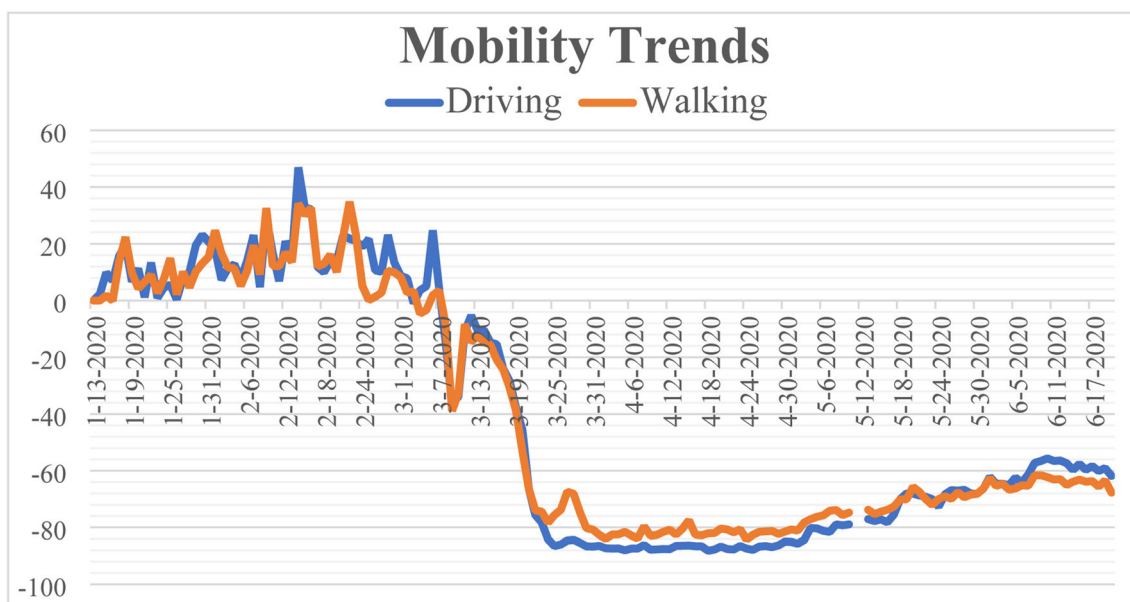


**Fig. 5** Mobility report for Delhi, India, from 15.02.2020 to 20.06.2020 for different places such as retail, grocery stores, parks, transit stations, workplaces and residential complexes. (Apple Mobility Reports, [52])

(Figs. 2, 3, 4, 5). Similar trends for decrease in air pollutants particularly,  $PM_{2.5}$  and  $PM_{10}$ , were found associated with human mobility trend in Singapore, during COVID-19 lockdown [53].

Since outdoor pollution concentrations also affect indoor pollution, people living inside their houses were also exposed to outdoor concentrations along with those going outdoors. Studies confirmed that outdoor PM concentrations can easily enter buildings and vehicles affecting their respective indoor quality [54, 55]. According to a research carried out in Germany, both outdoor and indoor  $PM_{2.5}$  levels were found well correlated with each other with significant correlation coefficient ( $r = 0.82$ ) whereas, similar results for correlations of outdoor and indoor PM were observed in Guangzhou and Beijing City of China [56–58]. Studies reported that indoor PM concentrations were found similar to the outdoor ones when the influence of other indoor sources is minimum. Modelling studies of  $PM_{2.5}$  suggested that absence of indoor sources, may be linked with the 50–70% presence of the outdoor  $PM_{2.5}$  concentrations at indoors [55, 59]. According to an Oxford study, in the presence of indoor activities like cleaning, cooking or smoking, PM concentrations exposure can even exceed than that of outdoor concentrations exposure [60]. Indoor sources like cleaning, dusting, walking, use of other domestic or office equipment, painting, smoking, etc. can increase PM concentrations at indoors [61, 62]. According to study of Birmingham, Wales and Cornwall, high concentrations of  $PM_{10}$  found indoors with their chemical composition also affected by the sources which were

present outdoors [63, 64]. Therefore, living indoors is also affected by outdoor concentrations of pollutants depending on meteorological conditions, ventilation systems present in the house and specific polluting sources at indoors.

Also, poor ventilation system and super-spreader events like large gatherings at indoors, may act as an enhancer for increase in COVID cases with increase in fine PM acting as a carrier for droplet transport. If indoor is heavily crowded with people along with poor air circulation in building, increase in their physical activity like loud talking, playing, laughing, singing and dancing can cause higher breathing rate, thus, increasing the number of micro-droplets release leading to high spread rate of viruses via respiratory droplets [3, 65]. According to Kay [66], super-spreader events play a major role in the faster spread of coronavirus and he has made an international database for Indian cities in a comprehensive way. The database consists of a list of major super-spreading events including large clusters for COVID-19 infection for a period including February and March 2020. The study suggested that most of the coronavirus infections outbreak were linked to indoor conditions where people were closely packed at the places like home, social gathering, workplace, public transport and restaurants [66]. According to another study, top 50 coronavirus outbreaks occurred at the large gatherings including events and places like weddings, funerals, religious places, prison, call centres, food packing centres, networking events related to business, etc. [3].



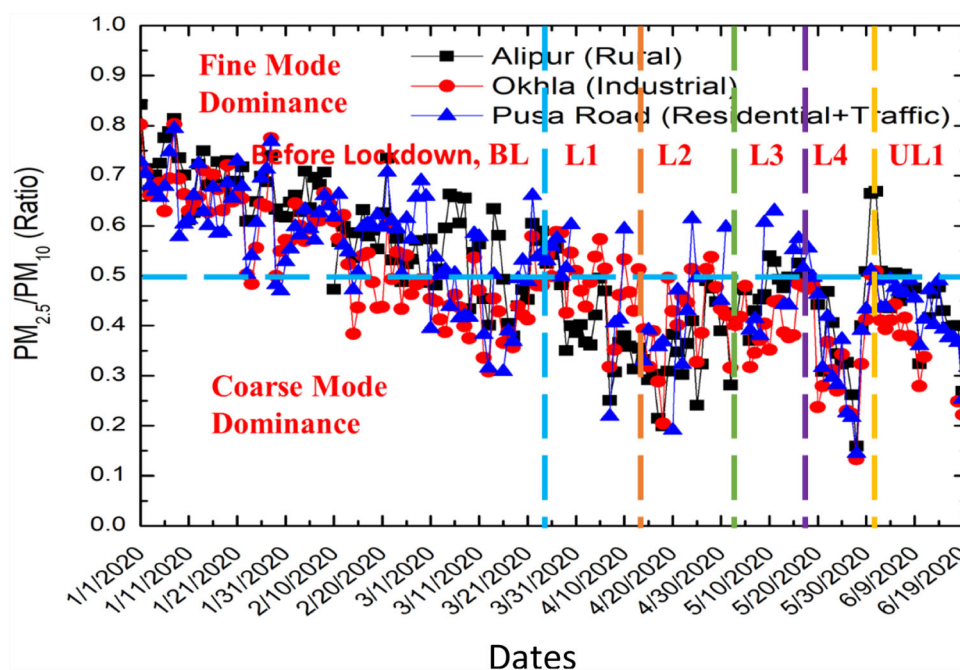


**Fig. 6** Daily variations in PM<sub>2.5</sub>/PM<sub>10</sub> ratio for three different sites identified by their region-specific signatures: **a** Alipur, **b** Okhla, **c** Pusa Road before, during and after lockdown phases

### 3.3. Variation in PM<sub>2.5</sub>/PM<sub>10</sub> Ratio Before and During COVID-19 Lockdown

PM<sub>2.5</sub> and PM<sub>10</sub> have different sources of emissions/generation, therefore, PM<sub>2.5</sub>/PM<sub>10</sub> ratio shows different characteristics of particle pollution, although, the ratio greatly varies at both spatial and temporal scale due to time and site-specific changes in PM concentrations. Mean values of PM<sub>2.5</sub>/PM<sub>10</sub> ratio are given in Table 1. The present study shows PM<sub>2.5</sub>/PM<sub>10</sub> ratio before lockdown as 0.54 ( $\pm 0.10$ ,  $\pm 0.11$ ) for both Alipur and Okhla sites and 0.48 ( $\pm 0.10$ ) for Pusa Road site, while L1 showed PM<sub>2.5</sub>/PM<sub>10</sub> ratio as 0.40 ( $\pm 0.08$ ) for Alipur, 0.48 ( $\pm 0.07$ ) for Okhla and 0.47 ( $\pm 0.12$ ) for Pusa Road, respectively (Table 1). Before lockdown, for Pusa Road and Okhla PM<sub>2.5</sub>/PM<sub>10</sub> ratio found  $> 0.5$  showing dominance of fine-sized particles with higher contribution from anthropogenic emissions, while at Alipur, the ratio was 0.48 ( $\pm 0.10$ ) showing dominance of coarse-sized particles than the fine particles (Table 1). At all the three sites fine mode particles were mostly dominant before lockdown condition with PM<sub>2.5</sub>/PM<sub>10</sub> ratio up to 0.80 while during lockdown coarse mode particles become dominant (Fig. 6). Higher ratios of PM<sub>2.5</sub>/PM<sub>10</sub> show contribution of anthropogenic sources in the particle pollution, whereas, smaller PM<sub>2.5</sub>/PM<sub>10</sub> ratios show presence of more coarse-sized particles in particle pollution, majorly emitted/generated from natural sources like dust storm [24]. Higher PM<sub>2.5</sub>/PM<sub>10</sub> ratio in Delhi,

before lockdown, at Okhla site is attributed to nearby Industrial activities, at Pusa Road it is due to higher traffic density and at Alipur site, it is due to localized agricultural and landfill burning activities along with more or less vehicular emissions at all the three sites. Highest variation in PM<sub>2.5</sub>/PM<sub>10</sub> ratio observed at Okhla and Alipur sites due to presence of more complex and changing PM sources at these sites than at the Pusa Road site. According to a study conducted in three east-central US states, fine particles (PM<sub>2.5</sub>) are found to contribute 67% of coarse particles (PM<sub>10</sub>) whereas, study on 20 European areas showed average PM<sub>2.5</sub>/PM<sub>10</sub> ratio as 0.60 [67, 68]. In Saudi Arabia, average PM<sub>2.5</sub>/PM<sub>10</sub> ratio is found as 0.33 mainly due to contribution of coarse particles (sand/dust) from desert area [69]. According to a study conducted in the USA, higher PM<sub>2.5</sub>/PM<sub>10</sub> ratios were observed in the eastern ( $\sim 0.7$ ) part than the central or western ( $\sim 0.5$ ) parts of the USA [70]. Urban sites of Wuhan, China showed highest ratio as 0.75 during winter and lowest in summer as 0.55 [71]. Higher PM<sub>2.5</sub>/PM<sub>10</sub> ratio reported during winter or autumn than in summer or spring [71, 72] mainly due to increase in fine particles emissions or secondary aerosol formation due to higher fuel consumption for domestic and industrial heating and lower mixing height, during winters [38, 73]. Also, stable atmospheric conditions during winter cause wet and dry deposition of aerosols which favours accumulation of fine particles in the atmosphere due to which fine particles become dominant in PM<sub>10</sub>, during winter

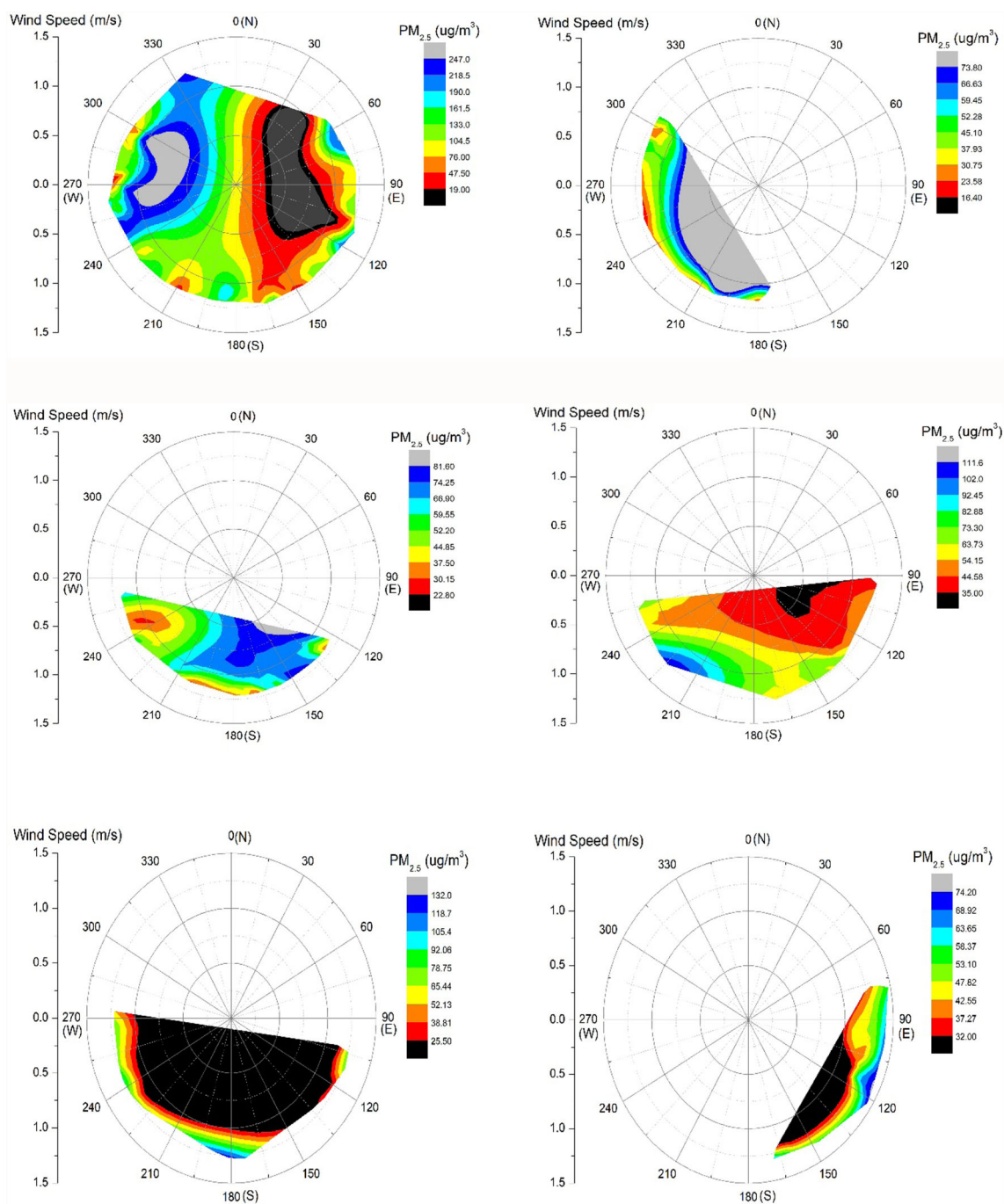


**Fig. 7** Polar plots of the hourly variations in wind speed (round radius, in units of m/s) and direction (angles) to surface  $PM_{2.5}$  concentrations (colour contours, in units of  $\mu g/m^3$ ) at Alipur, Delhi **a** from 01.01.2020 to 24.03.2020 (Before Lockdown, BL), **b** from

25.03.2020 to 14.04.2020 (Lockdown 1, L1), **c** from 15.04.2020 to 03.05.2020 (Lockdown 2, L2), **d** from 04.05.2020 to 17.05.2020 (Lockdown 3, L3), **e** from 18.05.2020 to 31.05.2020 (Lockdown 4, L4), **f** from 01.06.2020 to 20.06.2020 (Unlock 1, UL1)

[39].  $PM_{2.5}/PM_{10}$  percentage (%) change from BL–L1, L1–L2, L2–L3, L3–L4, L4–UL1 is calculated as – 25.93, – 15, 41.18, – 18.75, – 7.69 for Alipur, – 11.11, – 16.67, 0, – 20, 31.25 for Okhla and – 2.08, – 6.38, 11.36, – 26.53, 22.22 for Pusa Road site, respectively.

### 3.4. Source Apportionment of PM ( $PM_{2.5}$ and $PM_{10}$ ) at Selected Sites—Alipur, Okhla and Pusa Road Before and During COVID-19 Lockdown

Polar Plots of  $PM_{2.5}$  concentrations have been plotted against wind speed and wind direction for BL, L1, L2, L3,

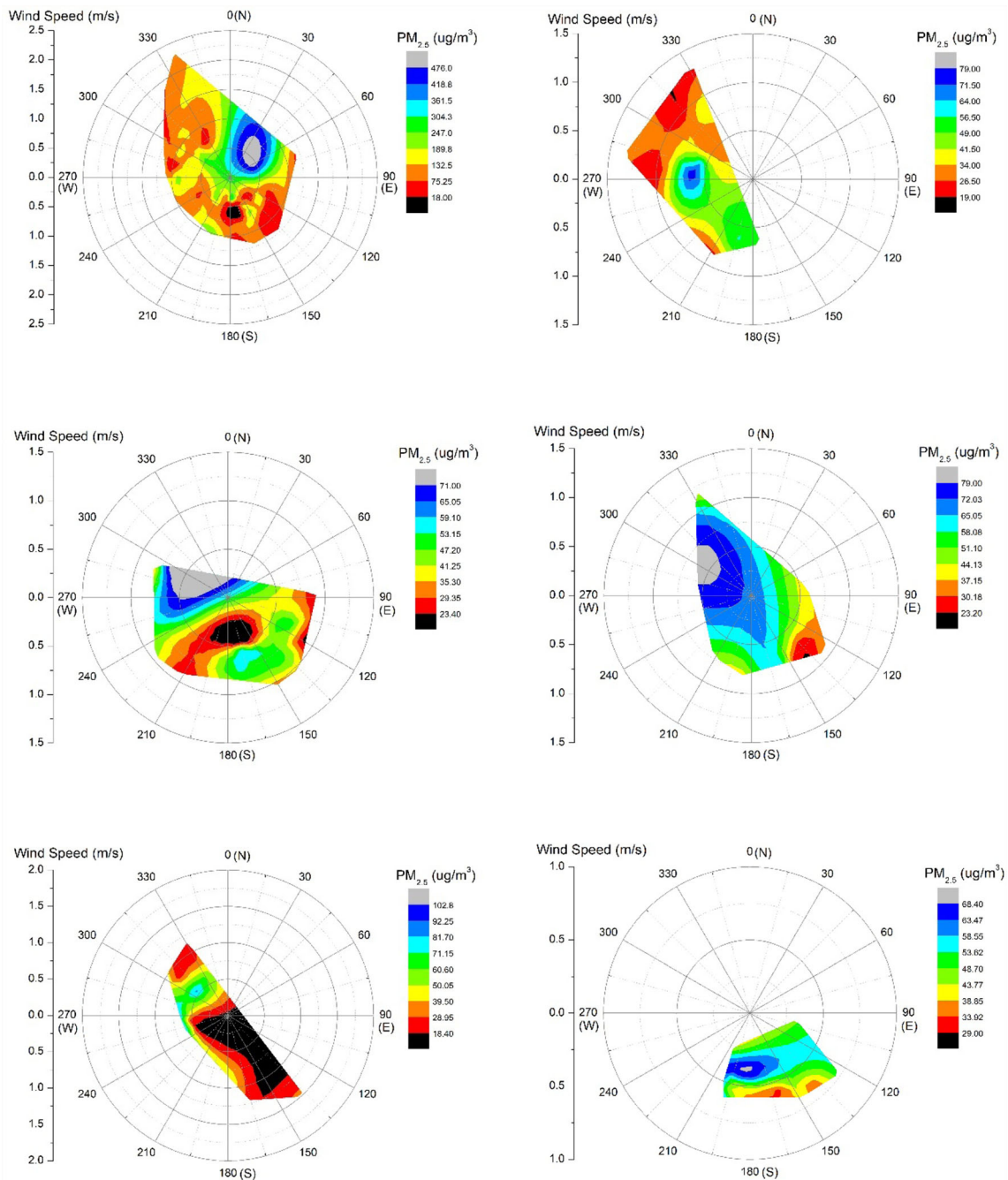


**Fig. 8** Polar plots of the hourly variations in wind speed (round radius, in units of m/s) and direction (angles) to surface PM<sub>2.5</sub> concentrations (colour contours, in units of  $\mu\text{g}/\text{m}^3$ ) at Okhla, Delhi **a** from 01.01.2020 to 24.03.2020 (Before Lockdown, BL), **b** from

25.03.2020 to 14.04.2020 (Lockdown 1, L1), **c** from 15.04.2020 to 03.05.2020 (Lockdown 2, L2), **d** from 04.05.2020 to 17.05.2020 (Lockdown 3, L3), **e** from 18.05.2020 to 31.05.2020 (Lockdown 4, L4), **f** from 01.06.2020 to 20.06.2020 (Unlock 1, UL1)

L4 and UL1 phases at all the three sampling sites (Figs. 7, 8, 9). Alipur, during BL phase, most of the higher concentrations were reported to coming from W and NW directions with wind speed varying between (0–0.5 m/s) showing dominance of local contribution of PM<sub>2.5</sub> sources mainly from vehicular emissions or local biomass burning activities (Fig. 7). Some higher PM<sub>2.5</sub> emissions were also

coming from N, S and SW directions with higher wind speed up to 1.25 m/s which shows both local and regional transfer of PM<sub>2.5</sub> at Alipur site. During L1, most of the higher concentration were associated with S, SW, W and NW with wind speed 0–1.25 m/s. Higher PM<sub>2.5</sub> concentrations were found with, SW and S directions with 0.25–1.25 m/s for L2; SW with 0.75 to 1 m/s for L3; S

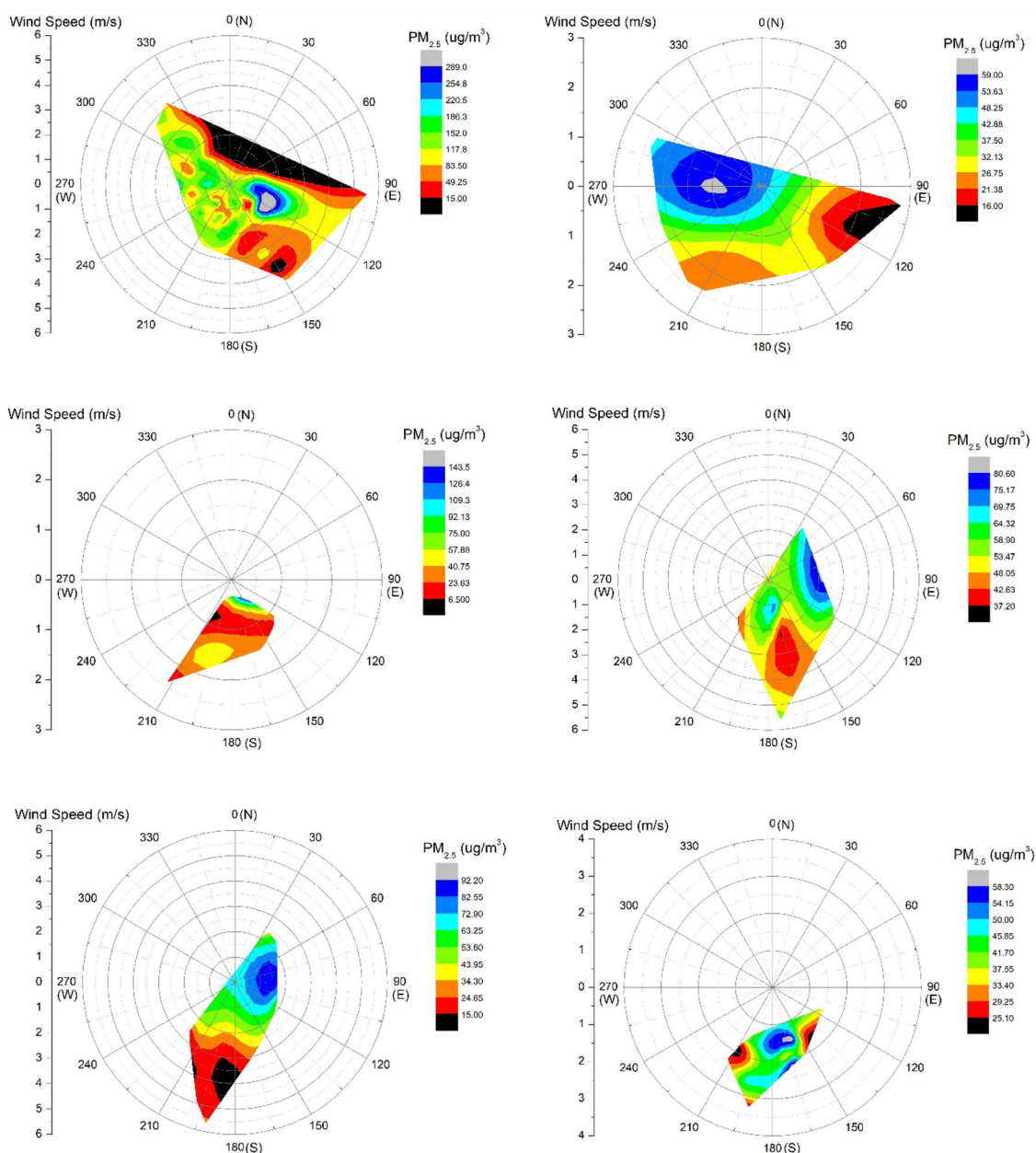


**Fig. 9** Polar plots of the hourly variations in wind speed (round radius, in units of m/s) and direction (angles) to surface  $PM_{2.5}$  concentrations (colour contours, in units of  $\mu g/m^3$ ) at Pusa Road, Delhi **a** from 01.01.2020 to 24.03.2020 (Before Lockdown, BL),

**b** from 25.03.2020 to 14.04.2020 (Lockdown 1, L1), **c** from 15.04.2020 to 03.05.2020 (Lockdown 2, L2), **d** from 04.05.2020 to 17.05.2020 (Lockdown 3, L3), **e** from 18.05.2020 to 31.05.2020 (Lockdown 4, L4), **f** from 01.06.2020 to 20.06.2020 (Unlock 1, UL1)

with 1–1.25 m/s for L3; and, SE with 0.25–0.75 m/s. Therefore, at Alipur, most of the higher concentrations were associated with S, SW, N, NW with wind speed varying between 0.25 and 1.25 m/s showing contribution of both local and regional  $PM_{2.5}$  sources (Fig. 7).

At Okhla, BL phase has higher  $PM_{2.5}$  Contribution from N and NE direction with lower wind speed 0–1 m/s showing effect of local emission sources like nearby Okhla industrial estate (Fig. 8). Higher  $PM_{2.5}$  concentrations were found associated with, W with 0–0.25 m/s wind speed

during L1; W and NW with 0–0.25 m/s wind speed during L2; W, NW and SW with 0–1 m/s wind speed during L3; W and SW with < 0.5 m/s wind speed during L4; and, S with 0.25–0.5 m/s wind speed during UL1 phase.  $PM_{2.5}$  pollution at Okhla was found mostly associated with lower wind speed 0–1 m/s confirms the local source contribution towards  $PM_{2.5}$  during different phases of study (Fig. 8).

At Pusa Road, higher  $PM_{2.5}$  concentrations were reported for E direction with 0–1 m/s wind speed during BL phase; W with 0–1 m/s wind speed during L1; S with

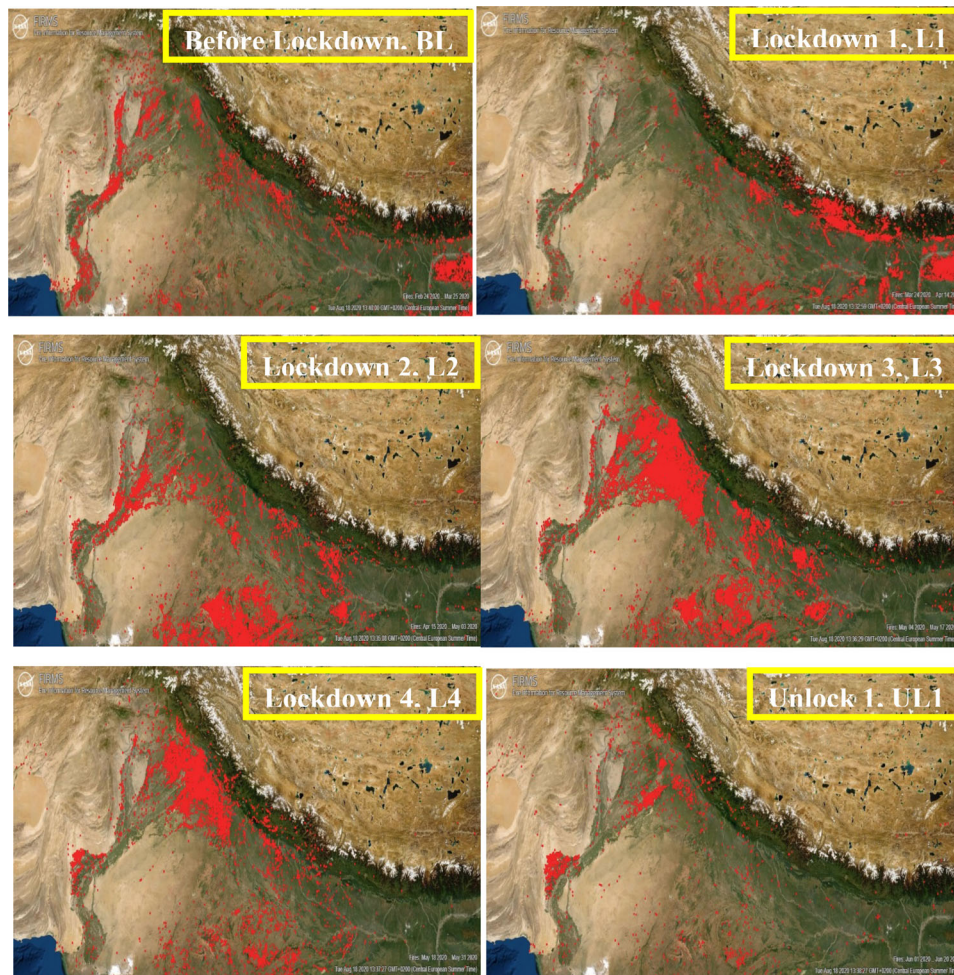


**Fig. 10** Fire counts map from 24.02.2020 to 20.06.2020 (BL, L1, L2, L3, L4 and UL1) showing major crop burning (CRB) events across Northern India in L3 and L4 phases during May 2020

0–0.5 m/s wind speed during L2; E and NE with 0–1 m/s wind speed during L3; E and NE with 0–1 m/s wind speed phase; and, S and SE with 2–3 m/s wind speed during UL1 phase (Fig. 9). Highest wind speeds up to 5.5 m/s has been reported at Pusa Road site mostly during L3 and L4 phase showing effect of regional contribution at this site during the mentioned lockdown period (Fig. 9). The strong near-surface wind causes the intensification of PM<sub>2.5</sub> during heavy air pollution periods [74].

Fire count data plots show major crop residue burning (CRB) events across Northern India during May 2020, i.e. during L3 and L4 phases (Fig. 10). Higher PM<sub>2.5</sub> concentration at Alipur rural site during L3 and L4 confirms the effect of CRB events in Delhi (Fig. 2). Figure 11 shows NOAA HYSPLIT wind trajectory plots for all the three sites, from 09.05.2020 to 15.05.2020 (for L3 phase)

duration. These wind trajectory plots confirmed the pollutants from fire events and wind during L3 phase found to be coming from areas where major crop burning (CRB) activities took place across Northern India thus affecting selected sampling sites for PM<sub>2.5</sub> pollution by regional transfer of pollutants from biomass burning activities during lockdown phases L3 and L4. The meteorological conditions of ambient atmosphere greatly affect atmospheric processes like transport, diffusion, dispersion, transformations and depositions of PM present in the atmosphere. The results of source apportionment studies confirm that wind direction in Delhi is a major factor with affects PM concentrations and acts as an indicator of the natural and anthropogenic sources and their locations present in the specific directions. Wind direction also affects temporal and seasonal variations of PM concentrations [75, 76].

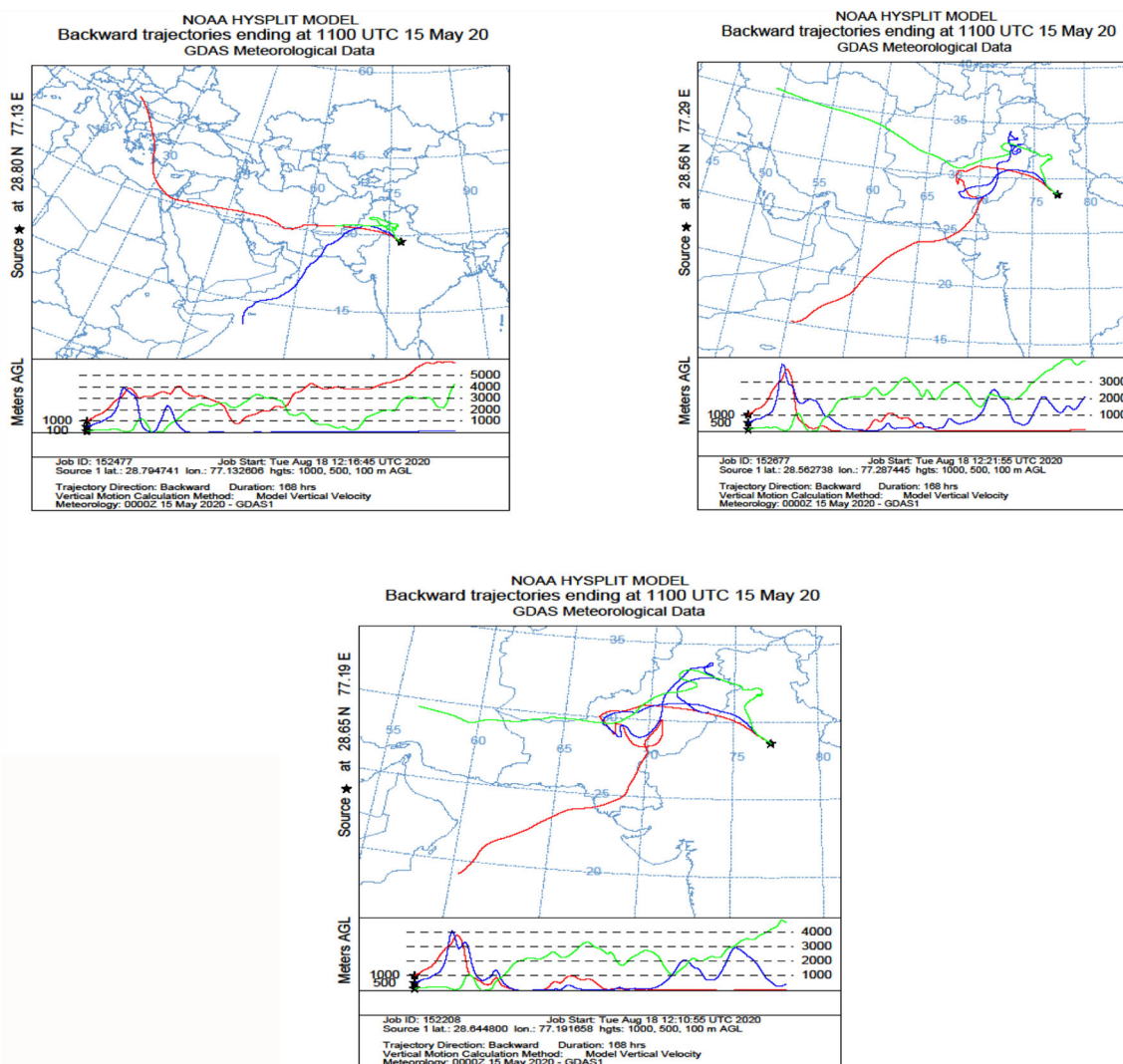


**Fig. 11** Wind trajectory plots from 09.05.2020 to 15.05.2020 (L3) supporting pollutants source from major crop burning (CRB) events across Northern India at **a** Alipur, **b** Okhla, **c** Pusa Road sites in Delhi

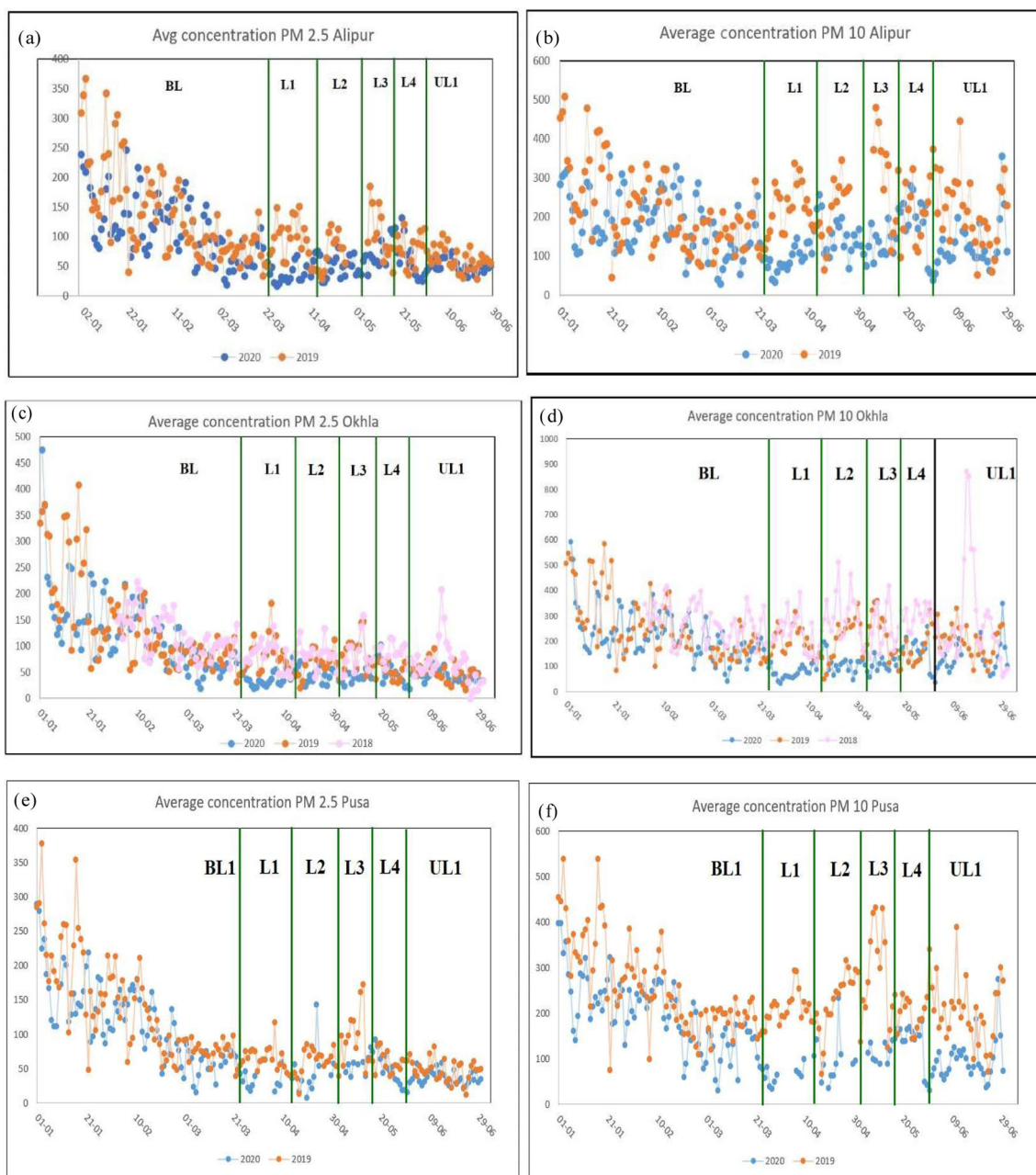
### 3.5. Comparison of PM Variations with that of 2018 and 2019

Figure 12 shows daily average concentrations ( $\mu\text{g}/\text{m}^3$ ) of  $\text{PM}_{2.5}$  and  $\text{PM}_{10}$  for three different sites—Alipur (fig: a and b), Okhla (fig: c and d), Pusa Road (fig: e and f), respectively, before, during and after lockdown phases (year 2020) and comparisons with that of the years 2018, 2019. The study suggests that 24 h average  $\text{PM}_{2.5}$  and  $\text{PM}_{10}$  concentrations are minimum for the year 2020 during various lockdown phases whiles the same is higher for 2018 and 2019 for the same period without lockdown conditions. This shows, in general, all the sampling sites chosen are greatly affected by the specific sources of air pollution without lockdown conditions as discussed in

previous sections of this paper. Similar comparison studies of lockdown period with pre-lockdown conditions for years 2019 and 2020 have been done by Chauhan and Singh [30] and Zhang et al. [33].

### 3.6. Comparison of PM Diurnal Variations During Various Lockdown Phases

Figure 13 shows diurnal variations of hourly average concentrations ( $\mu\text{g}/\text{m}^3$ ) of  $\text{PM}_{2.5}$  and  $\text{PM}_{10}$  for three different sites—Alipur (fig: a and b), Okhla (fig: c and d), Pusa Road (fig: e and f), respectively, before, during and after lockdown phases including BL, L1, L2, L3, L4, UL1 phases (year 2020). The comparison study confirms that Alipur site at 6.00 h of L4 shows highest average



**Fig. 12** Daily average concentrations ( $\mu\text{g}/\text{m}^3$ ) of PM<sub>2.5</sub> and PM<sub>10</sub> for three different sites—Alipur (fig: a and b), Okhla (fig: c and d), Pusa Road (fig: e and f), respectively, before, during and after lockdown phases (year 2020) and comparisons with the years 2018, 2019

concentration for both PM<sub>2.5</sub> and PM<sub>10</sub> may be due to biomass burning activities. Okhla site is characterized by highest PM<sub>2.5</sub> and PM<sub>10</sub> at 8.00 h for BL phase attributed by industrial activities during before lockdown conditions. Pusa Road site shows highest concentrations of both PM<sub>2.5</sub> and PM<sub>10</sub> during 2.00 h in L3 phase mainly due to haze events. Haze events were found to dominate Delhi region in L3 phase during night-time which increased PM<sub>2.5</sub> concentration as reported by Dhaka et al. [77].

#### 4. Summary and Conclusion

The findings of the study may be summarized as:

- The present study showed higher concentrations of both PM<sub>2.5</sub> and PM<sub>10</sub> concentrations at all the three selected sampling sites of Delhi—Alipur, Okhla, Pusa before lockdown (BL), which drastically decreased during Lockdown-1 (L1) phase. Gradual increase in concentrations for both pollutants at all the three sampling

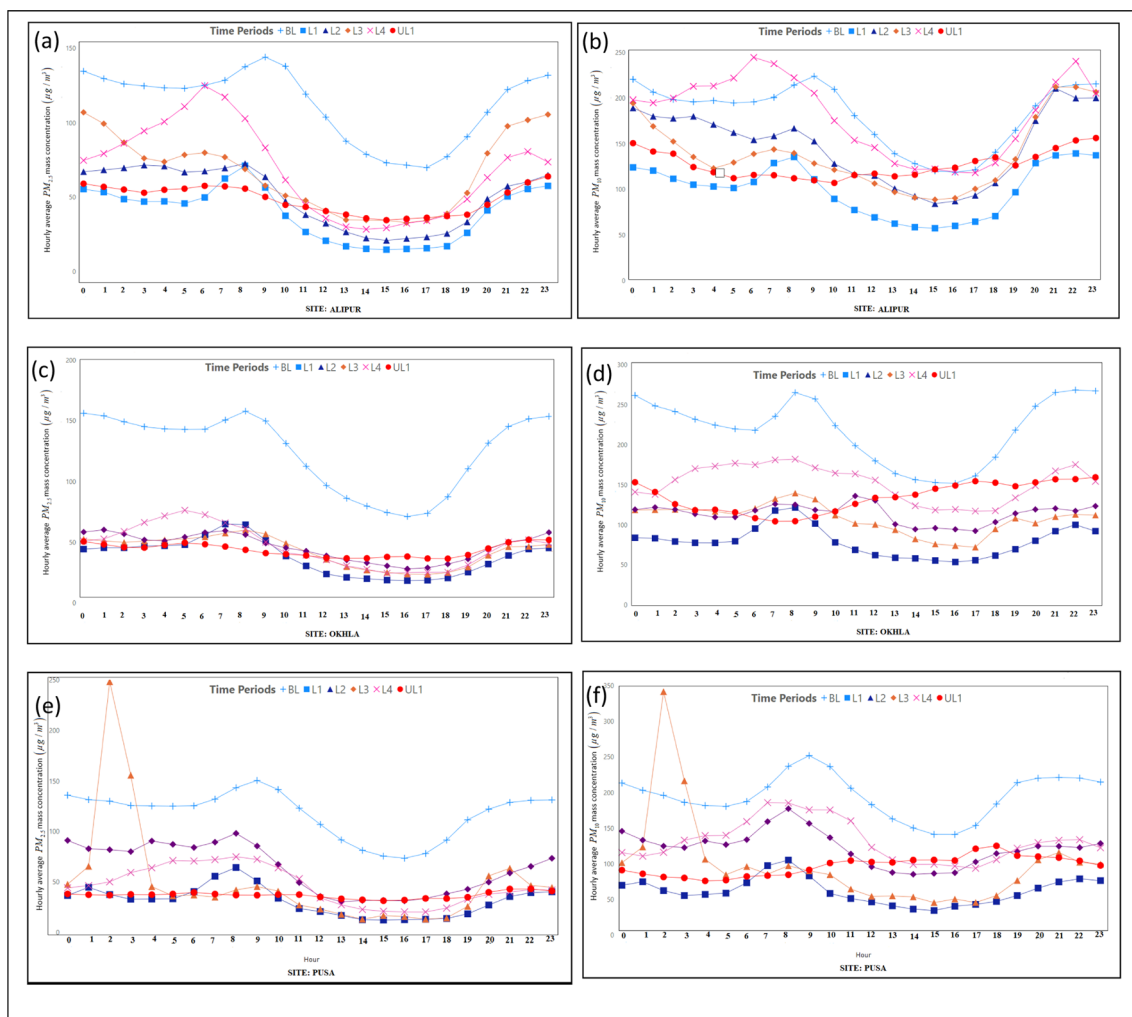


**Fig. 13** Diurnal variations of hourly average concentrations ( $\mu\text{g}/\text{m}^3$ ) of  $\text{PM}_{2.5}$  and  $\text{PM}_{10}$  for three different sites—Alipur (fig: **a** and **b**), Okhla (fig: **c** and **d**), Pusa Road (fig: **e** and **f**), respectively, before,

during and after lockdown phases including BL, L1, L2, L3, L4, UL1 phases (year 2020)

sites observed during successive lockdown phases including L2, L3, L4 and unlock phase—UL1. Highest % decrease at Okhla industrial site than other sites shows lesser industrial activities at this site during lockdown period whereas almost 50% decrease in PM concentrations at Pusa Road may be due to lesser traffic activities during lockdown period and lower % decrease in PM concentrations at Alipur may be attributed to lower but ongoing localized activities like agricultural burning, landfill burnings and lower emissions from vehicular emissions. At all the three sites fine mode particles were mostly dominant before lockdown condition with  $\text{PM}_{2.5}/\text{PM}_{10}$  ratio up to 0.80 while during lockdown coarse mode particles become dominant. Comparison of  $\text{PM}_{2.5}$  and  $\text{PM}_{10}$  concentrations for the year 2020 with that of 2018 and 2019 and study on diurnal variations of  $\text{PM}_{2.5}$  and  $\text{PM}_{10}$  also confirmed the discussed emission sources.

- The gradual decrease/increase in concentrations of both  $\text{PM}_{2.5}$  and  $\text{PM}_{10}$  were found well correlated with people mobility during successive lockdown phases. According to Google and Apple mobility reports, outdoor activities like visiting grocery stores, retails, parks, transit stations and workplaces have decreased during L1 (70–80%) and gradually increased in successive phases of lockdown and unlock phases with up to –20% during UL1 phase.
- Polar Plots of  $\text{PM}_{2.5}$  concentrations against wind speed and wind showed that specific wind directions and wind speeds are associated with most of the higher concentrations at all the three sampling sites. Fire count data plots showed major crop residue burning (CRB) events across Northern India during May 2020, i.e. during L3 and L4 phases. NOAA HYSPLIT wind trajectory plots for all the three sites also confirmed that the wind during L3 phase found to be coming from areas where



CRB activities took place across Northern India thus affecting selected sampling sites for PM<sub>2.5</sub> pollution by regional transfer of pollutants from biomass burning activities during lockdown phases L3 and L4.

**Acknowledgements** The authors acknowledge the Director, CSIR-National Physical Laboratory, New Delhi, India, for his motivation and support.

## References

1. WHO. 2020. (<https://www.who.int/emergencies/diseases/novel-coronavirus-2019>).
2. <https://worldmeters.info/coronavirus>.
3. E.S. Bromage, Coronavirus: here's how germs are spread and where you're most likely to catch them. May World Economic Forum (2020). <https://www.weforum.org/agenda/2020/05/coronavirus-covid19-exposure-risk-catching-virus-germs>.
4. N.A. Anjum, Good in the Worst: COVID-19 Restrictions and Ease in Global Air Pollution. Preprints (2020). <https://doi.org/10.20944/preprints202004.0069.v12020040069>.
5. S. Muhammad, X. Long and M. Salman, COVID-19 pandemic and environmental pollution: a blessing in disguise? *Sci. Total Environ.*, 728 (2020) 138820.
6. A.M. Shrestha, U.B. Shrestha, R. Sharma, S. Bhattarai, H.N.T. Tran, and M. Rupakheti, Lockdown caused by COVID-19 pandemic reduces air pollution in Cities Worldwide (2020).
7. J. Wang, K. Tang, K. Feng and W. Lv, High temperature and high humidity reduce the transmission of COVID-19. *SSRN Electron. J.* (2020). <https://doi.org/10.2139/ssrn.3551767>.
8. R.J. Isaifan, The dramatic impact of Coronavirus outbreak on air quality: has it saved as much as it has killed so far? *Glob. J. Environ. Sci. Manag.*, 6 (2020) 275–288.
9. G. He, Y. Pan and T. Tanaka, COVID-19, city lockdowns, and air pollution: evidence from China. *medRxiv* (2020). <https://doi.org/10.1101/2020.03.29.20046649>.
10. Q. Wang and M. Su, A preliminary assessment of the impact of COVID-19 on environment—a case study of China. *Sci. Total Environ.*, 728 (2020) 138915. <https://doi.org/10.1016/j.scitotenv.2020.138915>.
11. Y. Zhu, J. Xie, F. Huang and L. Cao, Association between short-term exposure to air pollution and COVID-19 infection: evidence from China. *Sci. Total Environ.* (2020). <https://doi.org/10.1016/j.scitotenv.2020.138704>.
12. M.F. Bashir, B. Ma, B. Komal, M.A. Bashir, D. Tan and M. Bashir, Correlation between climate indicators and COVID-19 pandemic in New York, USA. *Sci Total Environ*, 728 (2020) 138835.
13. T. Hammer, H. Gao, Z. Pan and J. WanG, Relationship between aerosols exposure and lung deposition dose. *Aerosol Air Qual. Res.*, 20 (2020) 1083–1093.
14. S. Mahato, S. Pal and K.G. Ghosh, Effect of lockdown amid COVID-19 pandemic on air quality of the megacity Delhi, India. *Sci. Total Environ.*, 730 (2020) 139086.
15. S. Sharma, M. Zhang, J. Gao, H. Zhang and S.H. Kota, Effect of restricted emissions during COVID-19 on air quality in India. *Sci. Total Environ.*, 728 (2020) 138878.
16. C.K. Chan and X. Yao, Air pollution in mega cities in China. *Atmos. Environ.*, 42 (2008) 1–42.
17. A.B. Tabinda, Q. Habib, A. Yasar, R. Rasheed, A. Mahmood and A. Iqbal, Ambient air quality of Faisalabad with relevance to the seasonal variations. *MAPAN-J. Metrol. Soc. India*, 35 (2020) 421–426.
18. X. Querol, A. Alastuey, C.R. Ruiz, B. Artiñano, H.C. Hansson, R.M. Harrison, E. Buringh, H.M. Ten Brink, M. Lutz, P. Bruckmann, P. Straehl and J. Schneider, Speciation and origin of PM<sub>10</sub> and PM<sub>2.5</sub> in selected European cities. *Atmos. Environ.*, 38 (2004) 6555.
19. Z. Li, P.K. Hopke, L. Husain, S. Qureshi, V.A. Dutkiewicz, J.J. Schwab, F. Drewnick and K.L. Demerjian, Sources of fine particle composition in New York city. *Atmos. Environ.*, 38 (2004) 6521–6529.
20. J. Suneja, G. Kotnala, A. Kaur, T.K. Mandal and S.K. Sharma, Long-term measurements of SO<sub>2</sub> over Delhi, India. *MAPAN-J. Metrol. Soc. India*, 35 (2019) 125–133.
21. G. Xu, L. Jiao, S. Zhao, M. Yuan, X. Li, Y. Han, B. Zhang and T. Dong, Examining the impacts of land use on air quality from a spatio-temporal perspective in Wuhan. *China. Atmos.*, 7 (2016) 62.
22. L.C.G. Blanco-Becerra, A.I. Afaro-Rojas and N.Y. Rojas-Roa, Influence of precipitation scavenging on the PM<sub>2.5</sub>/PM<sub>10</sub> ratio at the Kennedy locality of Bogota, Colombia. *Rev. Facul. Ing. Univ. Antioq.*, 76 (2015) 58–65.
23. A. Speranza, R. Caggiano, S. Margiotta and S. Trippetta, A novel approach to comparing simultaneous size segregated particulate matter (PM) concentration ratios by means of a dedicated triangular diagram using the Agri Valley PM measurements as an example. *Nat. Hazards Earth Syst. Sci.*, 14 (2014) 2727–2733.
24. N. Sugimoto, A. Shimizu, I. Matsui and M. Nishikawa, A method for estimating the fraction of mineral dust in particulate matter using PM<sub>2.5</sub>-to- PM<sub>10</sub> ratios. *Particuology*, 28 (2016) 114–120.
25. S. Munir, T.M. Habeebullah, A.M.F. Mohammed, E.A. Morsy, M. Rehan and K. Ali, Analysing PM<sub>2.5</sub> and its association with PM<sub>10</sub> and meteorology in the arid climate of Makkah, Saudi Arabia. *Aerosol Air Qual. Res.*, 17 (2017) 453–464.
26. D. Zhao, H. Chen, E. Yu and T. Luo, PM<sub>2.5</sub>/PM<sub>10</sub> ratios in eight economic regions and their relationship with meteorology in China. *Adv. Meteorol.* (2019). <https://doi.org/10.1155/2019/5295726>.
27. P. Salvador, B. Artiñano, M. Viana, A. Alastuey and X. Querol, Evaluation of the changes in the Madrid metropolitan area influencing air quality: analysis of 1999–2008 temporal trend of particulate matter. *Atmos. Environ.*, 57 (2012) 175–185.
28. J. Aldabe, D. Elustondo, C. Santamaria, et al., Chemical characterisation and source apportionment of PM<sub>2.5</sub> and PM<sub>10</sub> at rural, urban and traffic sites in Navarra (North of Spain). *Atmos. Res.*, 102 (2011) 191–205.
29. P. Kumar, I. Rivas and L. Sachdeva, Exposure of in-pram babies to airborne particles during morning drop-in and afternoon pick-up of school children. *Environ. Pollut.*, 224 (2017) 407–420.
30. A. Chauhan and R.P. Singh, Decline in PM<sub>2.5</sub> concentrations over major cities around the world associated with COVID-19. *Environ. Res.*, 187 (2020) 109634.
31. A.K. Srivastava, P.D. Bhojar, V.P. Kanawade, P.C.S. Devara, A. Thomas and V.K. Soni, Improved air quality during COVID-19 at an urban megacity over the Indo-Gangetic Basin: From stringent to relaxed lockdown phases. *Urban Clim.*, 36 (2021) 100791.
32. A. Thomas, V.P. Kanawade, C. Sarangi and A.K. Srivastava, Effect of COVID-Shutdown on aerosol direct radiative forcing over the Indo-Gangetic Plain out flow region of the Bay of Bengal. *Sci. Total Environ.*, 1 (2021) 1. <https://doi.org/10.1016/j.scitotenv.2021.146918>.
33. M. Zhang, A. Katiyar, S. Zhu, J. Shen, M. Xia, J. Ma, S.H. Kota, P. Wang and H. Zhang, Impact of reduced anthropogenic emissions during COVID-19 on air quality in India. *Atmos. Chem. Phys.*, 21 (2021) 4025–4037. <https://doi.org/10.5194/acp-21-4025-2021>.
34. <https://app.cpcbcr.com/ccr/#/caaqm-dashboard-all/caaqm-landing>.

35. <https://www.ready.noaa.gov>
36. <https://www.firms.modaps.eosdis.nasa.gov>
37. <https://earth.google.com>
38. R.J. Huang, Y. Zhang, C. Bozzetti, K.F. Ho, J.J. Cao, Y. Han, K.R. Daellenbach, J.G. Slowik, S.M. Platt, F. Canonaco, P. Zotter, R. Wolf, S.M. Pieber, E.A. Brun, M. Crippa, G. Ciarelli, A. Piazzalunga, M. Schwikowski, G. Abbazade, J. Schnelle-Kreis, R. Zimmermann, Z. An, S. Szidat, U. Baltensperger, I. El Haddad and A.S. Prevot, High secondary aerosol contribution to particulate pollution during haze events in China. *Nature*, 514 (2014) 218–222. <https://doi.org/10.1038/nature13774>.
39. W. Huang, E. Long, J. Wang, R. Huang and L. Ma, Characterizing spatial distribution and temporal variation of PM<sub>10</sub> and PM<sub>2.5</sub> mass concentrations in an urban area of southwest China. *Atmos. Pollut. Res.*, 6 (2015) 842–848.
40. A. Ahlawat, A. Wiedensohler and S.K. Mishra, An overview on the role of relative humidity in airborne transmission of SARS-CoV-2 in indoor environments. *Aerosol Air Qual. Res.*, 20 (2020) 1856–1861.
41. L.M. Casanova, J. Soyung, A.W. Rutala, D.J. Weber and M.D. Sobsey, Effects of air temperature and relative humidity on coronavirus survival on surfaces. *Appl. Environ. Microbiol.*, 76 (2010) 2712–2717. <https://doi.org/10.1128/AEM.02291-09>.
42. A. Chin, J.T.S. Chu, M.R.A. Perera and K.P.Y. Hui, Stability of SARS-CoV-2 in different environmental conditions. *Lancet Microbe*, 5247 (2020) 20036673.
43. M. Moriyama, W.J. Hugentobler and A. Iwasaki, Seasonality of respiratory viral infections. *Annu. Rev. Virol.*, 7 (2020) 83–101.
44. T. Stephanie, Optimize occupant health, building energy performance and revenue through indoor-air hydration. 19 November Atlanta: ASHRAE (2019).
45. S. Taylor, Using the Indoor Environment to Contain the Coronavirus, an engineering lesson gone viral. *ES Magazine* March (2020).
46. S. Taylor, Accepting airborne transmission of SARS-COV-2: our greatest fear and greatest opportunity. *ES Magazine* May (2020).
47. H. Chan, J.S. Malik Peiris, S.Y. Lam, L.L.M. Poon, K.Y. Yuen and W.H. Seto, The effects of temperature and relative humidity on the viability of the SARS coronavirus K. *Adv. Virol.* (2011). <https://doi.org/10.1155/2011/734690>.
48. W. Jingyuan, T. Ke, F. Kai, and L. Weifeng, High temperature and high humidity reduce the transmission of COVID-19. *SSRN* (2020).
49. M. Yueling, Z. Yadong, L. Jiangtao, H. Xiaotao, W. Bo, F. Shihua, et al., Effects of temperature variation and humidity on the mortality of COVID-19 in Wuhan (2020). <https://doi.org/10.1101/2020.03.15.2003642>.
50. R. Velraj and R. Haghighat, The contribution of dry indoor built environment on the spread of Coronavirus: data from various Indian states. *Sustain. Cities Soc.*, 62 (2020) 102371.
51. <https://www.google.com/covid19/mobility>.
52. <https://www.apple.com/covid19/mobility>.
53. J. Li and F. Tartarini, Changes in air quality during the COVID-19 lockdown in Singapore and associations with human mobility trends. *Aerosol Air Qual. Res.*, 20 (2020) 1748–1758.
54. S. Holgate, J. Grigg, H. Arshad, N. Carslaw, P. Cullinan, S. Dimitroulopoulou, A. Greenough, M. Holland, B. Jones, P. Linden, T. Sharpe, A. Short, B. Turner, M. Ucci, S. Vardoulakis, H. Stacey, L. Hunter, A report on “The inside story: health effects of indoor air quality on children and young people” published by Royal society of Physicians and Royal College of Paediatrics and Child Health in January (2020)
55. J. Taylor, C. Shrubsole, P. Symonds, I. Mackenzie and M. Davies, Application of an indoor air pollution meta-model to a spatially-distributed housing stock. *Sci. Total Environ.*, 667 (2019) 390–399.
56. H. Huang, S.C. Lee, J.J. Cao, C.W. Zou, X.G. Chen and S.J. Fan, Characteristics of indoor/outdoor PM<sub>2.5</sub> and elemental components in generic urban, roadside and industrial plant areas of Guangzhou city, China. *J. Environ. Sci.*, 19 (2007) 35–43. [https://doi.org/10.1016/S1001-0742\(07\)60006-0](https://doi.org/10.1016/S1001-0742(07)60006-0).
57. R. Xu, X. Qi, G. Dai, H. Lin, J. Shi, C. Tong, P. Zhai, C. Zhu, L. Wang and A. Ding, A comparison study of indoor and outdoor air quality in Nanjing, China. *Aerosol Air Qual. Res.* (2019). <https://doi.org/10.4209/aaqr.2019.10.0496>.
58. L. Zhao, C. Chen, P. Wang, Z. Chen, S. Cao, Q. Wang, G. Xie, Y. Wan, Y. Wang and B. Lu, Influence of atmospheric fine particulate matter (PM<sub>2.5</sub>) pollution on indoor environment during winter in Beijing. *Build. Environ.*, 87 (2015) 283–291. <https://doi.org/10.1016/j.buildenv.2015.02.008>.
59. C. Dimitroulopoulou, M.R. Ashmore, M.T.R. Hill, M. Byrne and R. Kinnersley, INDAIR: a probabilistic model of indoor air pollution in the U.K. *Atmos. Environ.*, 40 (2006) 6362–6379.
60. H.K. Lai, H. Ferrier, M. Kendall and I. Myers, Personal exposures and microenvironment concentrations of PM<sub>2.5</sub>, VOC, NO<sub>2</sub> and CO in Oxford, UK. *Atmos. Environ.*, 38 (2004) 6399–6410.
61. M. Fazlzadeh, R. Rostami, S. Hazrati and A. Rastgu, Concentrations of carbon monoxide in indoor and outdoor air of Ghalyun cafes. *Atmos. Pollut. Res.*, 6 (2015) 550–555. <https://doi.org/10.5094/APR.2015.061>.
62. M. Stranger, S. Potgieter-Vermaak and R. Van Grieken, Comparative overview of indoor air quality in Antwerp, Belgium. *Environ. Int.*, 33 (2007) 789–797. <https://doi.org/10.1016/j.envint.2007.02.014>.
63. K.A. BeruBe, K.J. Sexton, T.P. Jones and T. Moreno, The spatial and temporal variations in PM<sub>10</sub> mass from six UK homes. *Sci. Total Environ.*, 324 (2004) 41–53.
64. N. Jones, C. Thornton, D. Mark, R. Harrison, Indoor/outdoor relationships of particulate matter in domestic homes with roadside, urban and rural locations (2000).
65. W. Chen, N. Zhang, J. Wei, H.-L. Yen and Y. Li, Short-range airborne route dominates exposure of respiratory infection during close contact. *Build. Environ.*, 176 (2020) 106859. <https://doi.org/10.1016/j.buildenv.2020.106859>.
66. J. Kay, COVID-19 superspreader events in 28 countries: critical patterns and lessons, Quillette (2020). <https://quillette.com/2020/04/23/covid-19-superspreader-events-in-28-countries-critical-patterns-and-lessons/>.
67. M. Eeftens, M.Y. Tsai, C. Ampe, B. Anwander, R. Beelen, T. Bellander, G. Cesaroni, M. Cirach, J. Cyrys, K. de Hoogh, A. De Nazelle, F. de Vocht, C. Declercq, A. Dédélé, K. Eriksen, C. Galassi, R. Gražulevičienė, G. Grivas, J. Heinrich, B. Hoffmann, M. Iakovides, A. Ineichen, K. Katsouyanni, M. Korek, U. Krämer, T. Kuhlbusch, T. Lanki, C. Madsen, K. Meliefste, A. Møller, G. Mosler, M. Nieuwenhuijsen, M. Oldenwening, A. Pennanen, N. Probst-Hensch, U. Quass, O. Raaschou-Nielsen, A. Ranzi, E. Stephanou, D. Sugiri, O. Udvardy, É. Vaskövi, G. Weinmayr, B. Brunekreef and G. Hoek, Spatial variation of PM<sub>2.5</sub>, PM<sub>10</sub>, PM<sub>2.5</sub> absorbance and PM coarse concentrations between and within 20 European study areas and the relationship with NO<sub>2</sub>—results of the escape project. *Atmos. Environ.*, 62 (2012) 303–317.
68. W.J. Parkhurst, R.L. Tanner, F.P. Weatherford, R.J. Valente and J.F. Meagher, Historic PM<sub>2.5</sub>/PM<sub>10</sub> concentrations in the south-eastern united states- potential implications of the revised particulate matter standard. *J. Air Waste Manag. Assoc.*, 49 (1999) 1060–1067.
69. M. Khodeir, M. Shamy, M. Alghamdi, M. Zhong, H. Sun, M. Costa, L.C. Chen and P.M. Maciejczyk, Source apportionment and elemental composition of PM<sub>2.5</sub> and PM<sub>10</sub> in Jeddah City, Saudi Arabia. *Atmos. Pollut. Res.*, 3 (2012) 331–340.

70. USEPA, Air quality criteria for particulate matter (final report, Oct 2004). U.S. Environmental Protection Agency, Washington, DC (epa 600/p-99/002af-bf) (2004).
71. G. Xu, L. Jiao, B. Zhang, S. Zhao, M. Yuan, Y. Gu, J. Liu and X. Tang, Spatial and temporal variability of the PM<sub>2.5</sub>/PM<sub>10</sub> ratio in Wuhan, Central China. *Aerosol Air Qual. Res.*, *17* (2017) 741–751.
72. A. Speranza, R. Caggiano, S. Margiotta, V. Summa and S. Trippetta, A clustering approach based on triangular diagram to study the seasonal variability of simultaneous measurements of PM<sub>10</sub>, PM<sub>25</sub> and PM<sub>1</sub> mass concentration ratios. *Arab. J. Geosci.*, *9* (2016) 132.
73. L. Liu, J. Wei, Y. Li and A. Ooi, Evaporation, and dispersion of respiratory droplets from coughing. *Indoor Air* (2016). <https://doi.org/10.1111/ina.12297>.
74. C. Yu, T. Zhao, Y. Bai, L. Zhang, S. Kong, X. Yu, J. He, C. Cui, J. Yang, Y. You, G. Ma, M. Wu and J. Chang, Heavy air pollution with a unique “non-stagnant” atmospheric boundary layer in the Yangtze River middle basin aggravated by regional transport of PM<sub>2.5</sub> over China. *Atmos. Chem. Phys.*, *20* (2020) 7217–7230.
75. G. Coskuner, M.S. Jassim and S. Munir, Characterizing temporal variability of PM<sub>2.5</sub>/PM<sub>10</sub> ratio and its relationship with meteorological parameters in Bahrain. *Environ. Forensics*, *19* (2018) 315–326. <https://doi.org/10.1080/15275922.2018.1519738>.
76. S.A. Guerra, D.D. Lane, G.A. Marotz, R.E. Carter, C.M. Hohl and R.W. Baldauf, Effects of wind direction on coarse and fine particulate matter concentrations in southeast Kansas. *J. Air Waste Manag. Assoc.*, *56* (2006) 1525–1531.
77. S.K. Dhaka, Chetna, V. Kumar, V. Panwar, A.P. Dimri, N. Singh, P.K. Patra, Y. Matsumi, M. Takigawa, T. Nakayama, K. Yamaji, M. Kajino, P. Misra and S. Hayashida, PM<sub>25</sub> diminution and haze events over Delhi during the COVID-19 lockdown period: an interplay between the baseline pollution and meteorology. *Sci. Rep.*, *10* (2020) 13442.

**Publisher’s Note** Springer Nature remains neutral with regard to jurisdictional claims in published maps and institutional affiliations.